

# WFC3 Ambient-2 Testing: Calibration Subsystem Performance

---

S. Baggett  
May 4, 2007

---

## ABSTRACT

*This report summarizes the behavior of the calsystem in the UVIS, based upon the recent ambient calibration tests (April 2007) using the UVIS-2 detector. Due to schedule constraints, only a small subset of the nominal UVIS calsystem tests were run; no IR data were acquired. The illumination patterns and features observed in the tungsten and deuterium data are described and the characteristics of the flatfields are evaluated in light of the calsystem requirements. Based on the limited dataset, the UVIS calsystem, both tungsten and deuterium, satisfies the uniformity specification ( $< \text{factor of two}$  over the full field of view), meets the flux requirement ( $> 16.7 \text{ e}^-/\text{s}/\text{pix}$ ) for all but one filter (FQ437N quad filter+deuterium lamp at medium current yields  $\sim 12 \text{ e}^-/\text{s}/\text{pix}$ ), and fulfills the short-term stability needs (better than 1% over one hour).*

---

## Introduction

Internal flatfields for the UVIS and IR channels are provided via the calibration subsystem (calsystem), an optical stimulus integrated into WFC3 and designed to provide uniform illumination across the entire field of view of both channels. The calsystem data allow monitoring of the instrument (e.g., gain, shutter behavior, high-frequency changes to the flatfields) as well as provide a means of correcting ground calibrations for use on-orbit. There are four tungsten lamps in the calsystem which supply the visible and infrared flux, one lamp plus one backup for each channel though any lamp can be configured to be used with any channel (in the April 2007 tests, only lamp #1 was used). In addition, there is a

deuterium lamp (no backup) to provide UV flux. The UVIS light from the calsystem is directed towards the detector through a hole in the UVIS M2 mirror; the IR light from the calsystem is relayed to a reflective diffuser which is on a paddle attached to the Channel Select Mechanism: when the CSM is out of the external light path, the diffuser is in the IR beam path. The CEI specifications require that the calsystem provide 1) illumination uniform to better than a factor of two over the field of view, 2) stability over hour ( $<1\%$ /pixel) and year ( $<5\%$ ) timescales and repeatability (over a year) to  $\pm 50\text{K}$  color temperature, and 4) flux from 200-2000nm at the level of at least  $10\text{K e}^-$  in 10 minutes ( $\sim 16.7 \text{ e}^-/\text{s/pix}$ ) for all spectral elements.

This report summarizes the characteristics of the UVIS calsystem data taken during the April 2007 instrument-level testing and compares the results to the requirements. Due to schedule limitations, only a small subsection of the UVIS calsystem proposals were run and there are no data with which to evaluate longterm behavior; in addition, no IR data were acquired at this time because the IR detector can not be sufficiently cooled in room (ambient) conditions.

## Observations and Analysis

Table 3 in Appendix A summarizes the UVIS calsystem exposures examined; the image readout formats were the same: full-frame, four-amp, unbinned, nominal gain 1.5, default bias offset (setting 3,  $\sim 3000 \text{ DN}$ ), obtained April 2007 under ambient conditions with the UVIS-2 detector operating at  $-54\text{C}$ . The tungsten exposures were taken with lamp #1; the deuterium exposures were taken at medium current. All images were processed through calwf3, performing the overscan correction (BLEVCORR) only and using versions of CCDTAB and OSCNTAB generated in Mar 2005 and Nov 2003, respectively.

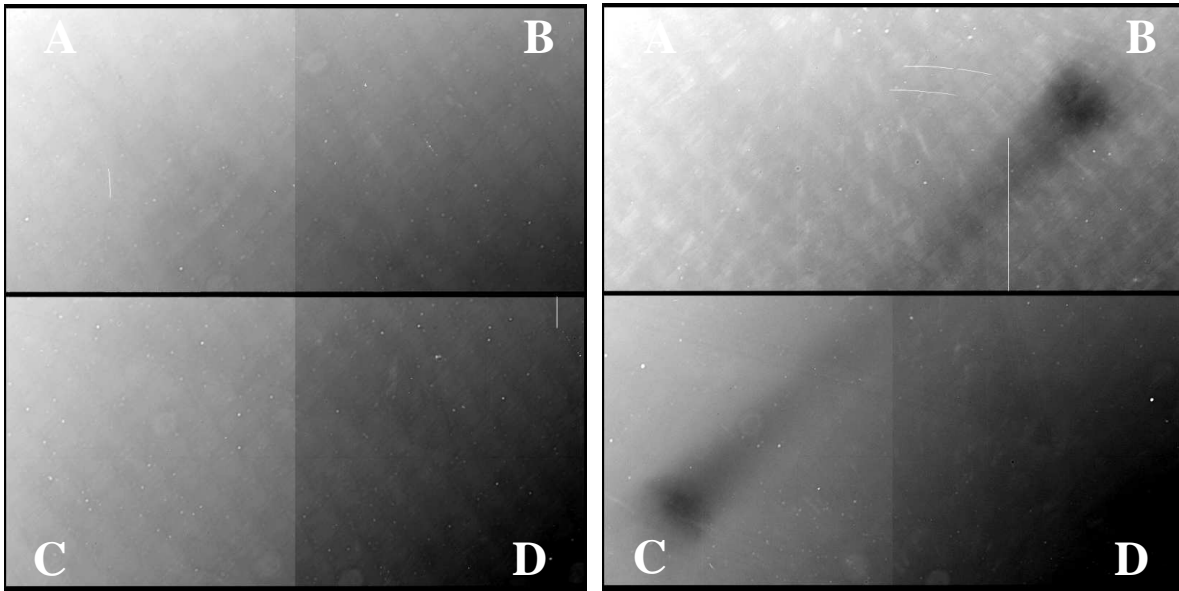
### *UVIS Tungsten Exposures*

#### *Image Features*

Tungsten calsystem images were obtained during April 2007 in six filters (F390W, F438W, F555W, F656N, F814W, and F953N). The new F390W image is shown in Figure 1, along with an older F390W calsystem flatfield taken in 2005. Immediately apparent is that the prominent ‘glints’ in quadrants B/C (connected by a broad swath of illumination) have been eliminated. Seen in calsystem flatfields taken during the first ground tests (Baggett, 2005), these features were found to be caused by a baffle that spans the distance between the SOFA and shutter in WFC3: the calsystem beam was hitting the baffle tube at glancing angles and being redirected onto the CCD (Turner-Valle 2005). Several possible methods of addressing this issue were discussed; the final solution implemented was to

roughen and paint the interior of the baffle with Martin black. As Figure 1 shows, the fix effectively eliminated the glints.

**Figure 1:** Full-frame, four-amp readout tungsten calsystem flatfields in F390W, shown with the same stretch ( $\pm 30\%$ ) with an inverted greyscale. At left is the most recent image, at right is an image taken in 2005, before the glint issue was identified and addressed. Quadrants in this figure, and all subsequent figures, are shown in the nominal position (labelled here with A,B,C,D).



For completeness, tungsten flatfields in all filters used during the April 2007 ambient testing are shown in Appendix B (best viewed on screen rather than on paper). The notable features are described in detail below.

- There is an overall gradient across the field of view, from the outer corner of quadrant A to the outer corner of quadrant D (e.g., F555W and F814W in Appendix B). During tests in 2005, the gradient was found to be filter-independent, present even without a filter in position, at the level of a factor of  $\sim 1.4$ - $1.6$  across the field of view. The recent flatfields show that the gradient has remained, at the level of a factor of  $\sim 1.5$  based upon image statistics of the outermost  $400 \times 400$  corner of A and D (the latter is brighter); specific flux and gradient levels as a function of filter are listed in Table 1. The cause of the gradient has not been identified but it may lie within the calsystem itself since it does not appear in flatfields taken using the external (CASTLE) stimulus.

- There is a flare in quadrant A that starts in the upper left and opens down to the lower right, extending into a faint diamond shape which extends across the field of view from the A quadrant to the D quadrant (see F814W image in Appendix B). This feature is more clearly seen in redder flatfields. The diamond is likely not calsystem-related: in UVIS-1 it was visible in external flatfields as well as in detector images taken prior to its integration into WFC3 (e.g., Pre-Ship Review slides 39-40, Sept 24, 2003). The flare does have more structure now with the UVIS-2 detector than it did in 2004/2005 with the UVIS-1 detector; the flare substructures are 1-3% brighter than the surrounding areas.
- There are small arc-shaped glints, one each in the outer corner of quadrants A, B, and D and a pair in the outer corner of quadrant C (see F814W image in Appendix B). They are similar to the arc-shaped glints seen in UVIS-1 during the first ground testing, though at slightly different positions in the field of view. In the new F555W tungsten flatfields, the arclets are ~0.5-1% brighter than the surrounding areas. They are not visible in external flatfields though similar arc features have been seen in images containing (heavily exposed) point sources.
- There is a small 'shadow' feature visible in the upper right of quadrant B (e.g., F814W flatfield). Given that the fringes in the F953N flatfield become very closely spaced in this region, this is not a true shadow but rather an area where the detection layer thickness in the CCD (and thus sensitivity) is changing rapidly.
- There are extended donut-like features, most prominent in F438W and F390W, which are due to particles on the filter; they range in size from about 150 to 250 pixels in diameter. Other, much smaller scale spots (around 10-40 pixels in diameter) are due to dust on the CCD windows.
- The crosshatch, or quilt, pattern seen in the UV tungsten flatfields is a normal feature of the detector structure in the UV. Paper copies of the new F390W tungsten flatfield in Figure 1 may appear to lack the crosshatching, but this is an artifact of the printing; the pattern is visible in on-screen images of both the old and new flatfield (as well as in the deuterium flatfields, discussed later).
- The narrowband images show fringing; this was expected at redder wavelengths, a result of interference within the detector layers. The effect is prominent in the F953N flatfield and visible in F656N as well.

### *Image Flux Levels*

Table 1 lists the flux levels measured in the UVIS tungsten calsystem flatfields from the April 2007 ambient testing. Shown are measurements from the high and low areas of the flatfields (400x400 regions in the outer corners of quadrants D and A, respectively). The last column lists the average of the median flux of the four quadrants. All exposure levels have been converted to  $e^-/s/pix$  using the UVIS-2 gain values of 1.58, 1.55, 1.65, 1.61 for A, B, C, and D, respectively (Baggett, 2007). Dark current has not been removed from the flatfields but its contribution is very low: 0.002-0.004  $e^-/s/pix$  (Hilbert, 2007). All flux levels easily meet the CEI specification of 16.7  $e^-/s/pix$ . Only a subset of filters were

observed with the calsystem during the April 2007 ambient tests but assuming the relative predicted exposure times are valid (Table in UVIS23 procedure), the remaining filters are expected to have flux levels that satisfy the requirement. Note that the results here have been based upon images taken with one lamp only (#1); the tungsten calsystem has four lamps, two for each channel. The nominal UVIS and IR calsystem proposals, expected to run in their entirety during the thermal-vacuum level tests scheduled for summer of 2007, contain a check of the flux levels and illumination patterns in each of the four lamps.

**Table 1.** UVIS tungsten lamp 1 calsystem exposure levels in the April 2007 images. Listed is image name, filter, exposure time, low flux (outer corner of A), high flux (outer corner of D), and average of the median fluxes of the four quadrants.

image	filter	exptime (sec)	flux (low corner) e <sup>-</sup> /s/pix	flux (high corner) e <sup>-</sup> /s/pix	gradient	full FOV ave flux e <sup>-</sup> /s/pix
iu23110ar_07107181410	F390W	550.	61.7	91.5	1.48	75.6
iu231109r_07107175946	F438W	335.	103.3	153.3	1.49	126.8
iu281d0cr_07110005853	F555W	10.	2184.0	3248.2	1.49	2702.1
iu281c0cr_07105045753	F555W	10.	2178.4	3238.7	1.49	2692.7
iu231104r_07107164920	F555W	14.	2185.7	3253.4	1.49	2704.3
iu231104r_07107172620	F555W	14.	2187.2	3254.0	1.49	2707.0
iu231105r_07107173951	F656N	480.	68.7	102.5	1.49	87.2
iu281d0dr_07110005853	F814W	1.5	16570.9	24453.0	1.48	20694.1
iu231102r_07107171219	F814W	1.9	16317.8	24091.3	1.48	20388.9
iu231102r_07107163519	F814W	1.9	16436.8	24278.1	1.48	20560.5
iu281c0dr_07105045753	F814W	1.5	16610.0	24534.2	1.48	20754.0
iu231107r_07107173951	F953N	65.	446.9	643.1	1.44	553.5

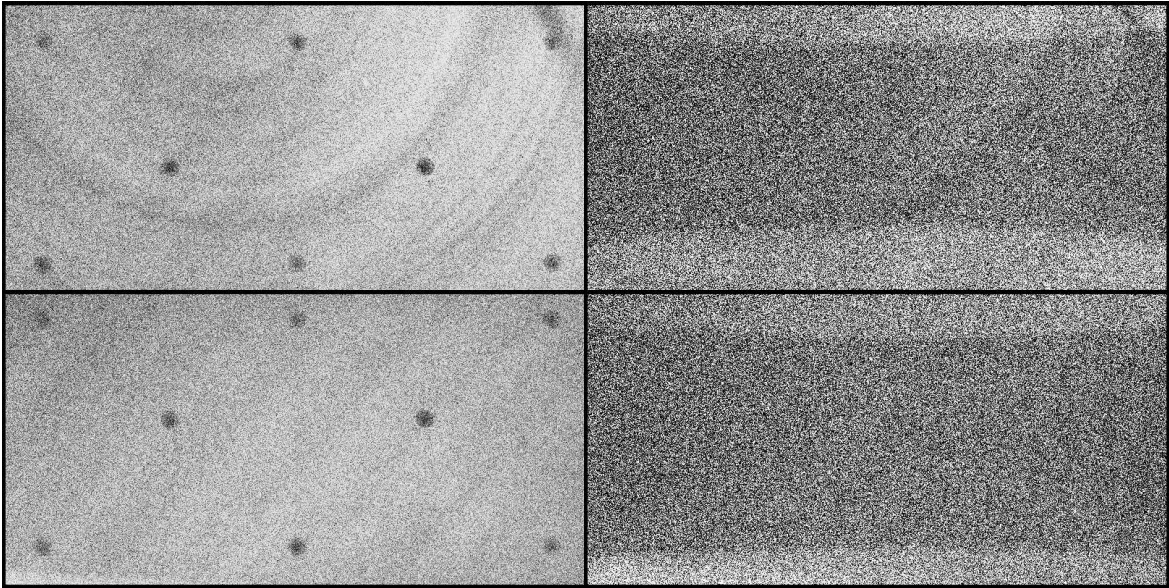
### *Tungsten Lamp Repeatability*

Two filters had more than one calsystem image taken during the ambient testing (F555W and F814W); in these cases, the lamp repeatability was found to be ~1% or better. That is, the full FOV flux of the individual F555W images were within -0.3 to +0.2% of the average full FOV flux of the set of 4 images; the full FOV flux of the individual F814W images were within -1.0 to +0.8% of the average full FOV flux of the set of 4 images.

Displays of the flatfield image ratios show what appears to be a low-level hysteresis-type features. The effect is currently being investigated in more depth; presented here is a short summary of the characteristics gleaned from the recent calsystem images. Two types of

patterns have been seen (see Figure 2): an extended, slowly curving, horizontal shape ('bowtie') and small extended PSF-like spots in a pattern matching the images taken for alignment measurements<sup>1</sup> ('field points'). Both types of patterns were also seen in the previous ground tests with the UVIS-1 detector. Typically noticeable in image ratios, it has also been seen occasionally in single images, most recently in a 900 sec dark taken with UVIS-2 on Mar 25, 2007.

**Figure 2:** Full frame calsystem F555W flatfield image ratios showing examples of the 'bowtie' (right) and 'field point' effect (left). Display is a hard inverted stretch (0.995 to 1.005) in order to highlight the features.



The level of the features is very low, ~0.1-0.5%, and in the calsystem flatfields, visible only in image ratios. The field point pattern was seen at ~0.5% (~100 e<sup>-</sup>) level in the ratio of an April 20 to an April 15 F555W flatfield, with the spots brighter on April 15 (closer in time to when the alignment data were acquired). The situation was similar for the F814W ratio (not shown) though the effect was much smaller than 0.5%; there was also some very faint diagonal striping from B down to C, possibly a shutter travel effect (G. Hartig, priv.comm.). The bowtie pattern was seen in the F555W ratio of two April 17 calsystem flatfields, one taken about 30 min earlier than the other. In this case, the bowtie area was

---

1. The alignment procedures obtain subarray images of a HeNe laser-generated point source as it is positioned at various predefined locations around the field of view. The standard pattern places the point source at 6 positions around the perimeter of each chip along with 1 position at the center of each quadrant (Hartig, 2003). A focus sweep - a set of images at a variety of focus settings - is obtained at each field point.

$\sim 0.1\%$  ( $\sim 40e^-$ ) brighter in the early image. Similarly, a ratio of two April 17 F814W flatfields taken about 30 min apart showed a bowtie pattern, with the central regions  $\sim 0.05\%$  ( $\sim 20 e^-$ ) brighter in the earlier image. The appearance of the small shadow-like area in the upper corner of quadrant B (discussed earlier) also seems to change over time, and in the same sense, as the bowtie and field point features.

### ***UVIS Deuterium Exposures***

#### *Image Features*

The new deuterium images are relatively flat, particularly in comparison to the images seen in the first ground testing which showed 5-10x gradients across the field of view from C quadrant up through B quadrant (Baggett, 2005). Figure 3 shows the new F390M flatfield; for completeness, the April 2007 deuterium flatfields obtained with other filters are included in Appendix C (best view on screen, rather than on paper). The new flatfields show that the gradient is largely gone though there is noticeably higher throughput in quadrants B and D near the center of the FOV. There is also some downturn in flux at the outer corners of quadrants B (20-40%), D (20-30%), and to a lesser extent, quadrant C ( $\sim 10\%$ ). The background cross-hatch pattern is part of the normal detector structure seen in UV flatfields, both calsystem and external; the sharply-outlined white spots seen in some flatfields (e.g., F300X) are normal as well: an effect of the painted pinholes in the inverted greyscale display. Disregarding the small spots and the extreme roll-offs at the edge which seem to be worse in redder filters, overall the deuterium flatfields meet the uniformity requirement (better than a factor of two across the field of view).

**Figure 3:** UVIS calsystem deuterium flatfield with F390M from April 2007. At left is the full field of view, scale is  $\pm 30\%$  with an inverted stretch; at right is a closeup of quadrant D with contour levels (2% intervals) overplotted to highlight the rolloff at the edge.

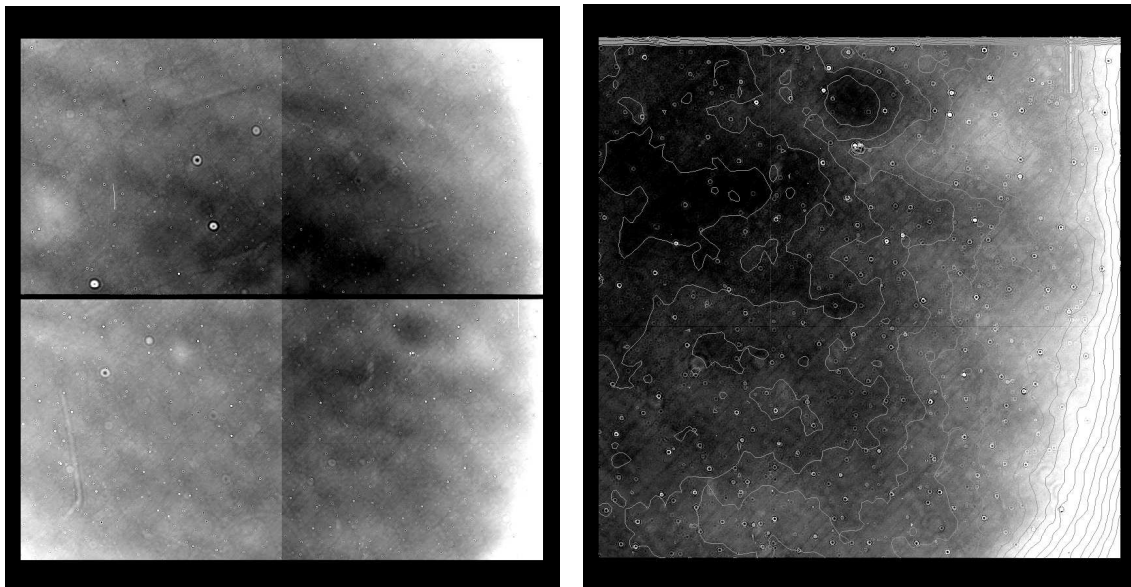


*Image Flux Levels*

The flux levels measured in the new deuterium calsystem flatfields are provided in Table 2 below. Listed are the image name, filter, exposure time, average flux in the higher flux area of quadrant B as well as an average of the median fluxes of all quadrants. Information for the quad filter has been broken into its four constituents (FQ437N, FQ378N, FQ232N, and FQ243N, in amps A,B,C, and D, respectively); “full FOV fluxes” in this case represent statistics from the appropriate quadrant. All exposure levels have been converted to  $e^-/s/pix$  using the UVIS-2 gain values for each quadrant (listed in tungsten flatfield section).

The flux requirement is met for all but the quad filter FQ437N (a relatively red bandpass for the deuterium lamp); its countrate is  $\sim 12 e^-/s/pix$  or about 70% of the specification. Using the tungsten lamp for this filter is not likely to improve the countrate unless the new tungsten lamps are significantly brighter than the old lamps; tungsten FQ437N flatfields taken with the previous generation of lamps had countrates of  $\sim 6 e^-/s/pix$  (no FQ437N tungsten flatfield was obtained during the short April 2007). Operating the deuterium lamp at the high current setting would double the countrate, thereby satisfying the specification. However, the results of a deuterium lamp lifetime study performed in the lab showed that the medium current setting minimized degradation in lamp performance and provided the most stable short and longterm throughput (Baggett and Quijada, 2003); for this reason, deuterium lamp operations are expected to be restricted to medium current only. Due to scheduling constraints, D2 flatfields were not taken in all UV filters; however, based upon the observed count rates and the predicted exposure times from procedure UV23, the D2 flatfields in the remaining filters should meet the flux requirement.

**Table 2.** UVIS deuterium lamp calsystem exposure levels in the April 2007 images; images were all taken at medium current. Columns list the image name, filter, exposure time, low flux (outer corner of A), high flux (outer corner of D), and average of the median fluxes of the four quadrants. For quad filters (FQ\*), full FOV flux is that of the appropriate quadrant for the filter listed.

image	filter	exptime (sec)	flux (high area in B) $e^-/s/pix$	full FOV ave flux $e^-/s/pix$
iu281d0fr_07110012206	F218W	24.	909.7	899.0
iu281c0fr_07105052106	F218W	24.	913.8	905.2
iu231508r_07109150011	F275W	46.7	1189.6	1126.4
iu231502r_07109135223	F300X	22.4	2274.1	2169.7
iu231505r_07109142634	F336W	78.	690.2	656.6



image	filter	exptime (sec)	flux (high area in B) e <sup>-</sup> /s/pix	full FOV ave flux e <sup>-</sup> /s/pix
iu23150dr_07109160702	F343N	150.	288.1	268.7
iu23150gr_07109163312	F390M	230.	146.9	138.1
iu23150ar_07109155009	F395N	2000.	--	>35 (est.) <sup>a</sup>
iu23150er_07109163312	FQ437N	1000.	--	11.9
	FQ378N		--	63.9
	FQ232N		--	56.7
	FQ243N		--	68.8
iu231507r_07109150011	FQ437N	1000.	--	12.1
	FQ378N		--	65.0
	FQ232N		--	57.7
	FQ243N		--	69.8
iu231504r_07109142634	FQ437N	1000.	--	12.1
	FQ378N		--	65.0
	FQ232N		--	57.9
	FQ243N		--	70.1

a. Flatfield in ambient was saturated; countrate is estimated to be at least 35 e<sup>-</sup>/s/pix assuming a conservative full well of 70K e<sup>-</sup>.

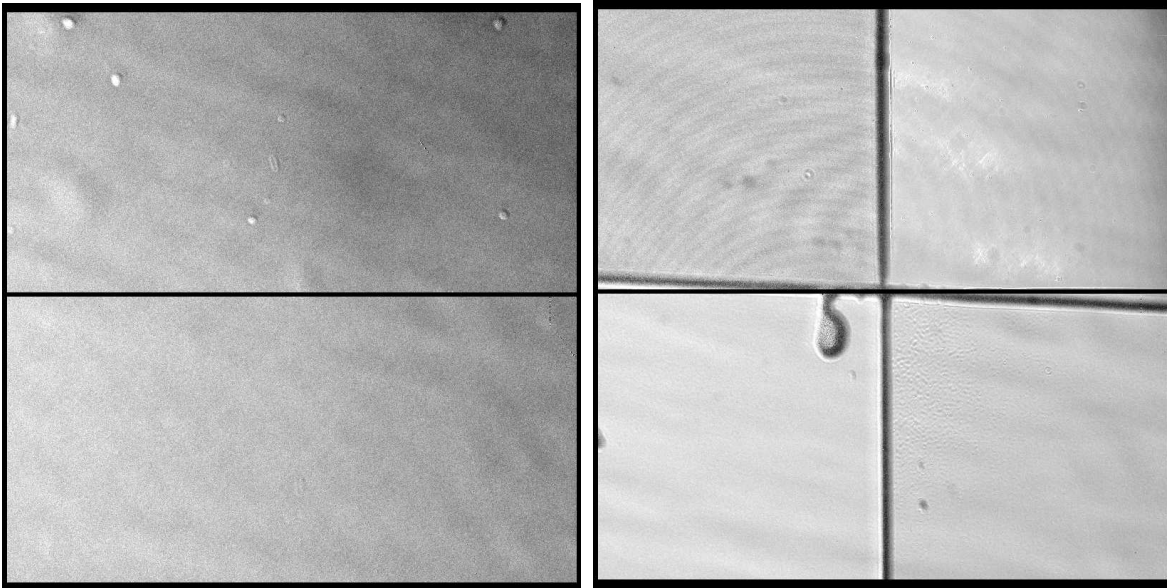
### *Deuterium Lamp Repeatability*

As with the tungsten lamp, the deuterium flatfields appear to be highly repeatable. Multiple calsystem flatfields were taken with two filters (F218W, FQ437N). In F218W, two flatfields were obtained; overall, the flux levels were within 0.5% of each other. The ratio image (see Figure 4) shows only extremely small variations, such as a slight ripple (<0.1%) from C to D quadrant and a slight change in intensity from lower left to upper right (<0.4%). There were some particles, seen as dark spots in quadrants A/B in Figure 3 (appearing as white in the inverted display scale), that seemed to have shifted position slightly from one flatfield to the next.

Three flatfields were obtained using one of the quad filters, a filter element where each quadrant is a different bandpass and each filter quadrant is imaged onto a different detector quadrant. In this case, the flatfields were taken with QUAD1, or FQ437N, FQ378N, FQ232N, and FQ243N, in amps A,B,C, and D, respectively. One of the image ratios is

shown in Figure 4; the prominent ‘+’ pattern is due to the boundaries between the four filter quadrants, where the individual glass segments for the different bandpasses were bonded together. The large spot in quadrant C is pinhole paint. While the majority of the ratio image is flat within each quadrant (to better than 1%), there are about a dozen small spots - the majority in quadrants A/B (FQ437N, FQ378N) - that appear in the ratio of image 3/1 (shown in Figure 4) that were not present in image 3/2 (not shown). There are some “ringing” or fringing type features as well. While prominent in the image display, the levels of the changes were generally small: few 0.1-0.5% ( $5\text{-}10e^-$ ) for the features in quadrant A and  $\sim 0.2\%$  ( $\sim 50e^-$ ) for features in quadrant C. The ratio image shows the spots as being brighter in the earlier image; they may be related to the phenomenon generating the ‘bowtie’ and fieldpoint patterns noted in the tungsten flatfield ratios.

**Figure 4:** Deuterium flatfield ratios for F218W (left) and FQ437N quad filter (right). Both are shown in inverted stretch, the former at  $\pm 2\%$  and the latter at  $\pm 3\%$ .



## Conclusions

The WFC3 calsystem flatfields from the April 2007 ambient tests with UVIS-2 have been examined and details of the illumination patterns discussed. Only a small subset of the calsystem proposals were run during this test but based upon this limited set of data, the UVIS tungsten and deuterium flatfields were found to meet the uniformity, flux (with exception of FQ437N, at  $\sim 12 e^-/s/pix$ ), and short-term stability requirements.

## Acknowledgements

Thanks are due to the WFC3 team members who made the ambient testing possible.

## References

- Baggett, S., “WFC3 Thermal Vacuum and Ambient Testing: Calibration Subsystem Performance,” WFC3 Instrument Science Report WFC3-2005-09, March 2005.
- Baggett, S., “WFC3 Ambient-2 Testing: UVIS Gain Results,” WFC3 Instrument Science Report WFC3-2007-11, April 2007.
- Baggett, S., and Quijada, M., “Lifetime Test of a Deuterium Lamp for the WFC3 Calibration Subsystem,” WFC3 Instrument Science Report WFC3-2003-11, November 2003.
- Hartig, G., “Image Positions for WFC3 Testing with CASTLE,” STScI Internal Memo, 15 May 2003.
- Hilbert, B., “WFC3 Ambient Testing: UVIS Dark Current Rate,” WFC3 Instrument Science Report WFC3-2007-10, April 2007.
- Turner-Valle, J., “UVIS Cal Subsystem Glints,” Ball Aerospace and Technologies Corp., April 2005.

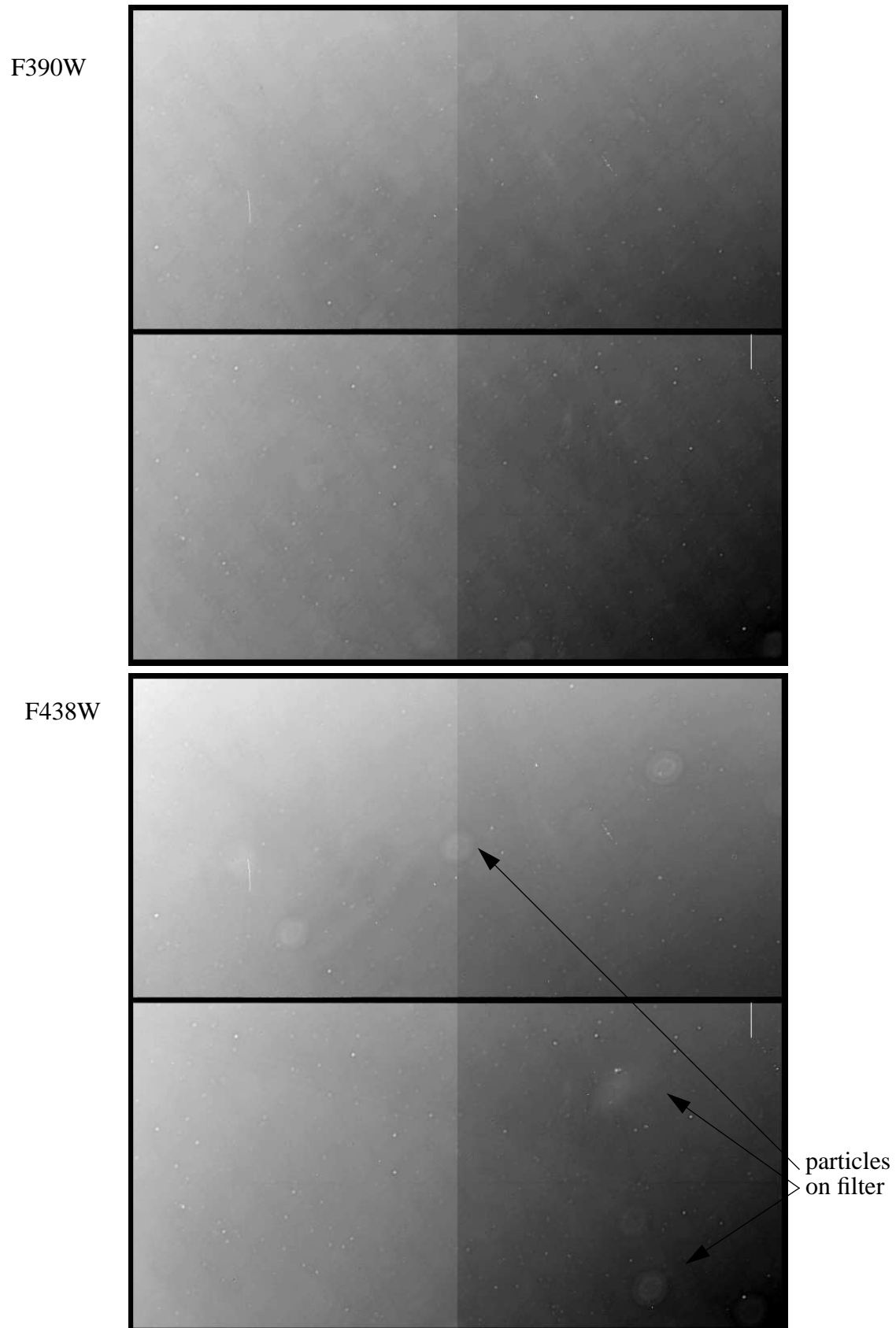
**Appendix A**

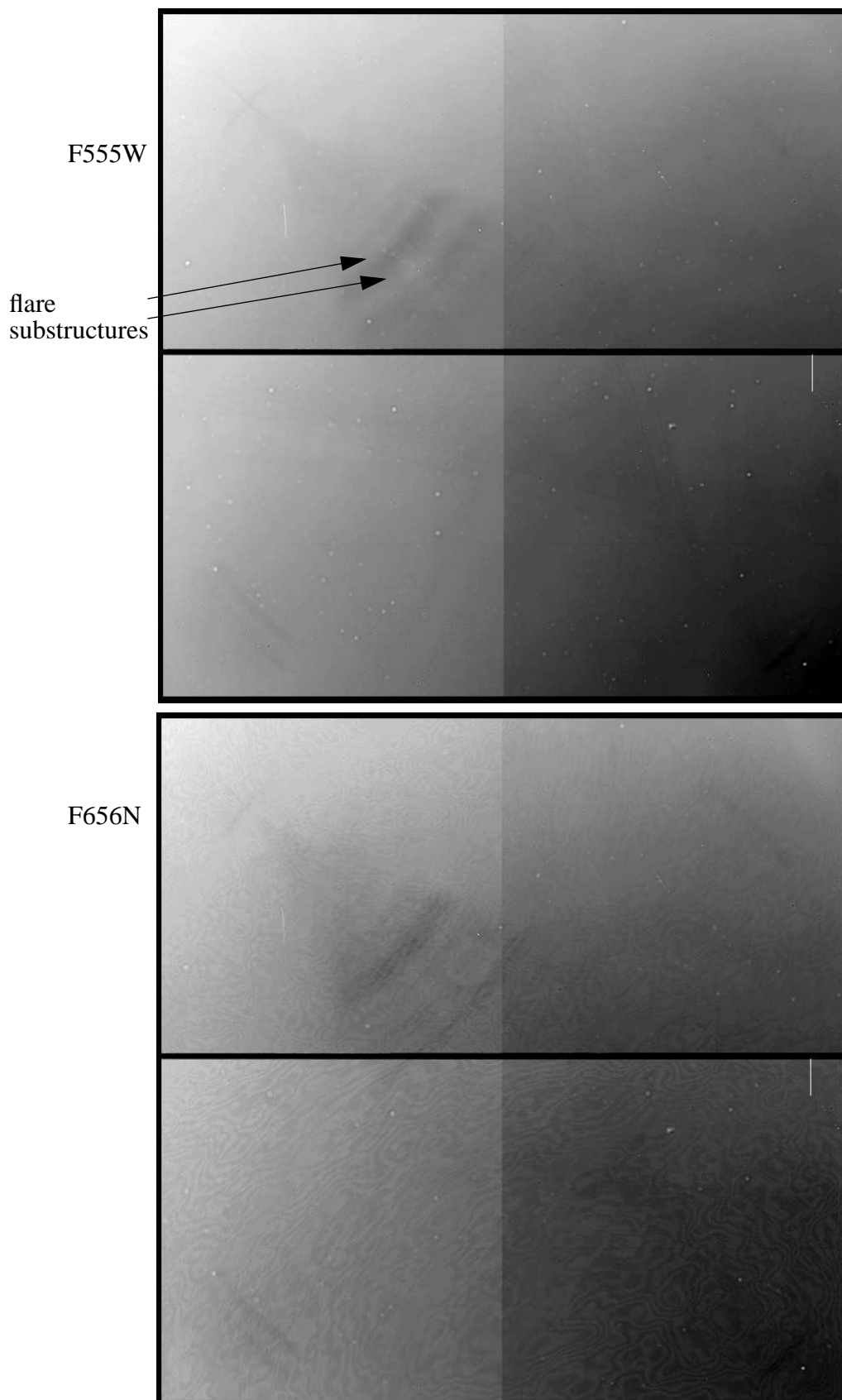
**Table 3.** List of April 2007 UVIS calsystem images analysed, along with the database entry number, rootname, lamp, filter, exposure time and date. All images were full-frame, four-amp, unbinned, nominal gain 1.5, default bias offset=3 readouts. The quad filter exposure (QUAD1) covers the four filters FQ437N, FQ378N, FQ232N, FQ243N in quadrants A,B,C, and D, respectively.

tv number	rootname	lamp	filter	exptime (sec)	start time
28937	iu231101r_07107163519	NONE	--	0. (bias)	2007-04-17 16:29:25
28940	iu231101r_07107171219	NONE	--	0. (bias)	2007-04-17 17:06:25
28938	iu231102r_07107163519	TUNGSTEN_LAMP1	F814W	1.9	2007-04-17 16:32:53
28941	iu231102r_07107171219	TUNGSTEN_LAMP1	F814W	1.9	2007-04-17 17:09:53
28939	iu231104r_07107164920	TUNGSTEN_LAMP1	F555W	14.	2007-04-17 16:46:22
28942	iu231104r_07107172620	TUNGSTEN_LAMP1	F555W	14.	2007-04-17 17:23:22
28943	iu231105r_07107173951	TUNGSTEN_LAMP1	F656N	480.	2007-04-17 17:25:55
28944	iu231107r_07107173951	TUNGSTEN_LAMP1	F953N	65.	2007-04-17 17:36:23
28945	iu231109r_07107175946	TUNGSTEN_LAMP1	F438W	335.	2007-04-17 17:51:18
28946	iu23110ar_07107181410	TUNGSTEN_LAMP1	F390W	550.	2007-04-17 17:59:21
28947	iu23110cr_07107181410	NONE	--	0. (bias)	2007-04-17 18:10:58
28997	iu231501r_07109135223	NONE	--	0. (bias)	2007-04-19 13:46:23
28998	iu231502r_07109135223	DEUTERIUM	F300X	22.4	2007-04-19 13:49:36
28999	iu231504r_07109142634	DEUTERIUM	QUAD1	1000.	2007-04-19 14:03:44
29000	iu231505r_07109142634	DEUTERIUM	F336W	78.	2007-04-19 14:22:52
29001	iu231507r_07109150011	DEUTERIUM	QUAD1	1000.	2007-04-19 14:37:52
29002	iu231508r_07109150011	DEUTERIUM	F275W	46.7	2007-04-19 14:57:00
29003	iu23150ar_07109155009	DEUTERIUM	F395N	2000.	2007-04-19 15:11:20
29004	iu23150br_07109155009	NONE	--	0. (bias)	2007-04-19 15:47:09
29005	iu23150dr_07109160702	DEUTERIUM	F343N	150.	2007-04-19 16:01:33
29006	iu23150er_07109163312	DEUTERIUM	QUAD1	1000.	2007-04-19 16:06:37
29007	iu23150gr_07109163312	DEUTERIUM	F390M	230.	2007-04-19 16:25:45
28367	iu281c0cr_07105045753	TUNGSTEN_LAMP1	F555W	10.	2007-04-19 04:51:56
28368	iu281c0dr_07105045753	TUNGSTEN_LAMP1	F814W	1.5	2007-04-19 04:54:28
28369	iu281c0fr_07105052106	DEUTERIUM	F218W	24.	2007-04-19 05:09:14
29019	iu281d0cr_07110005853	TUNGSTEN_LAMP1	F555W	10.	2007-04-20 00:52:56
29020	iu281d0dr_07110005853	TUNGSTEN_LAMP1	F814W	1.5	2007-04-20 00:55:28
29021	iu281d0fr_07110012206	DEUTERIUM	F218W	24.5	2007-04-20 01:10:14

## Appendix B

**Figure 5:** UVIS calsystem tungsten flatfields taken during ambient testing in April 2007. Shown with inverted greyscale and arbitrary hard stretch to highlight features.





F814W  
flare/diamond  
feature outlined

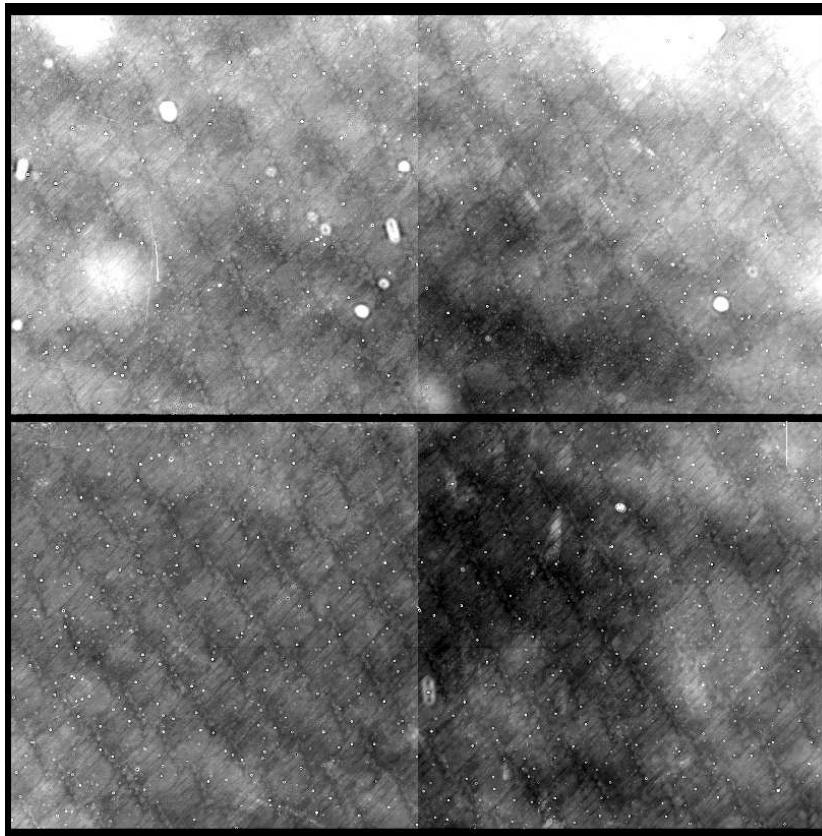
“shadow”  
feature

“arclet”  
glints

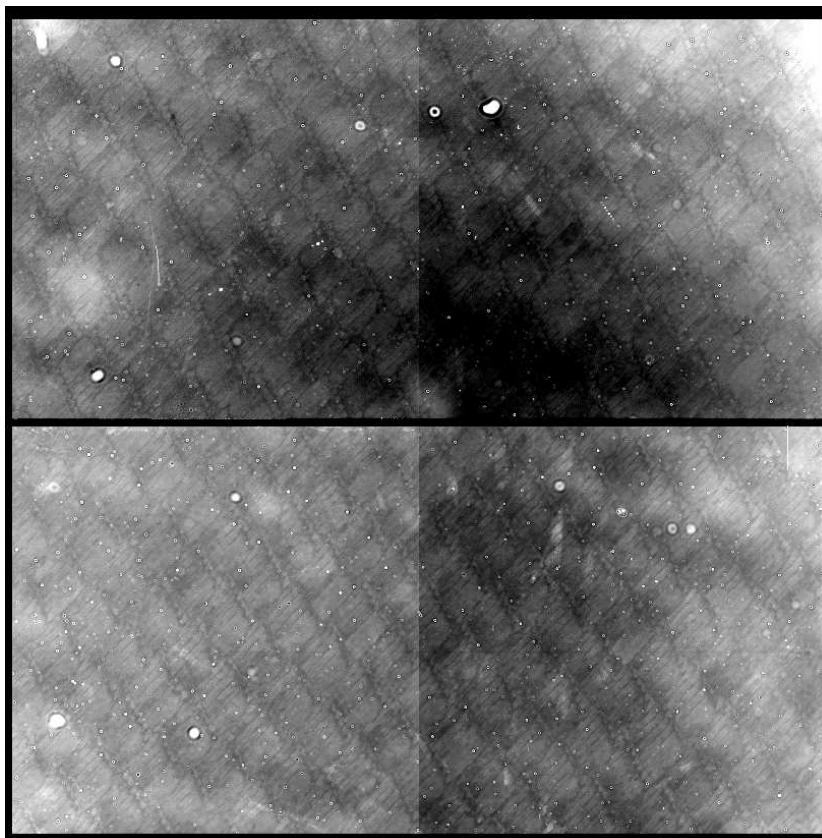
F953N

**Figure 6:** UVIS deuterium calsystem flatfields taken during ambient testing in April 2007. Shown with inverted greyscale and arbitrary hard stretch to highlight features.

F218W  
D2

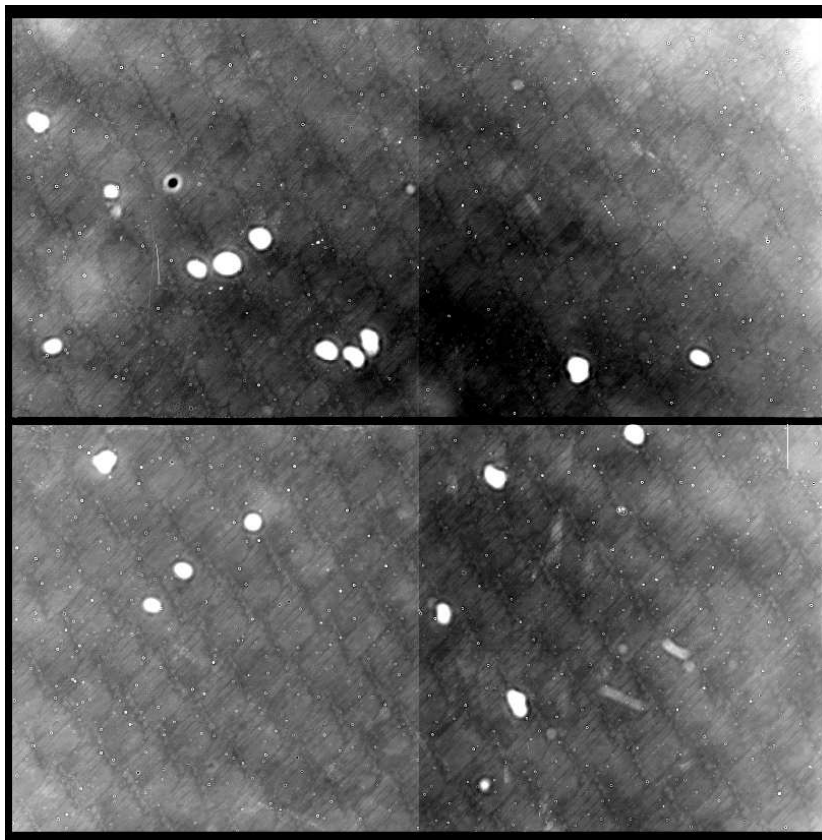


F275W  
D2

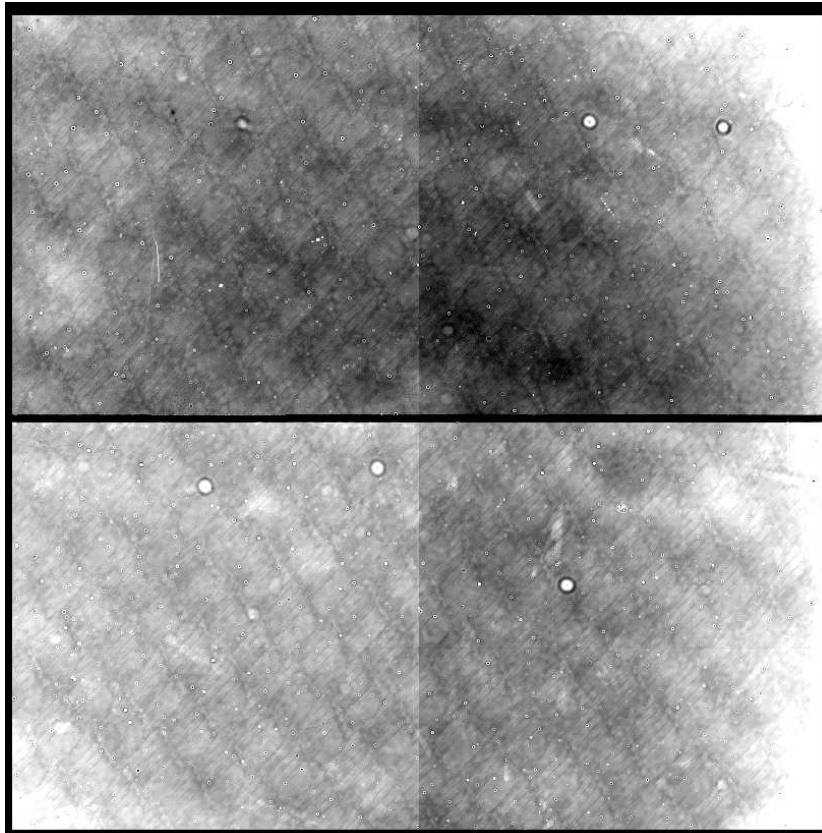




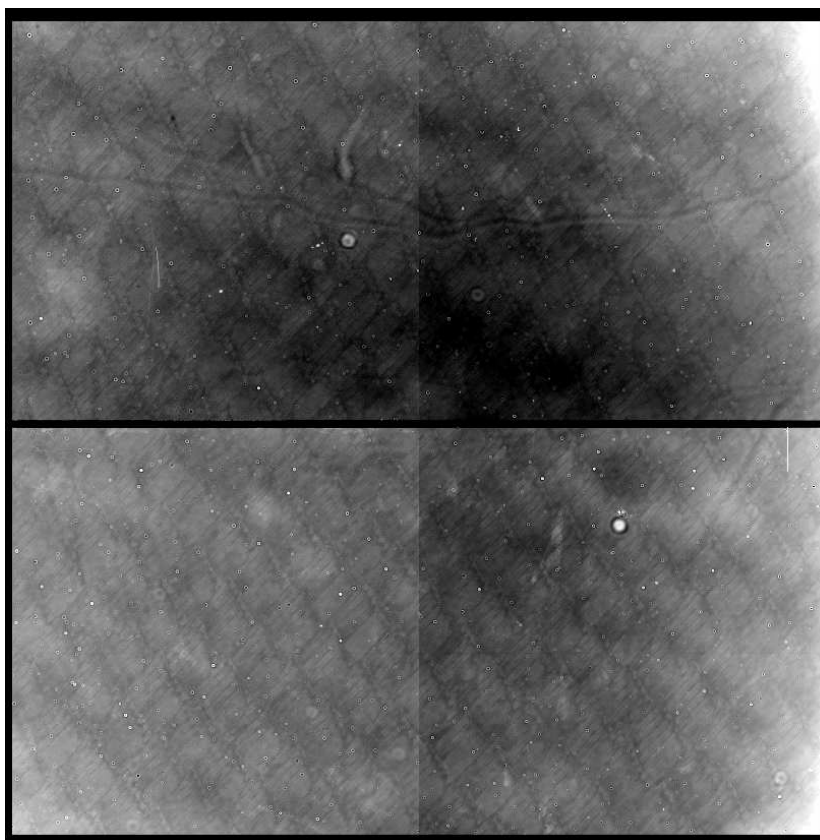
F300X  
D2



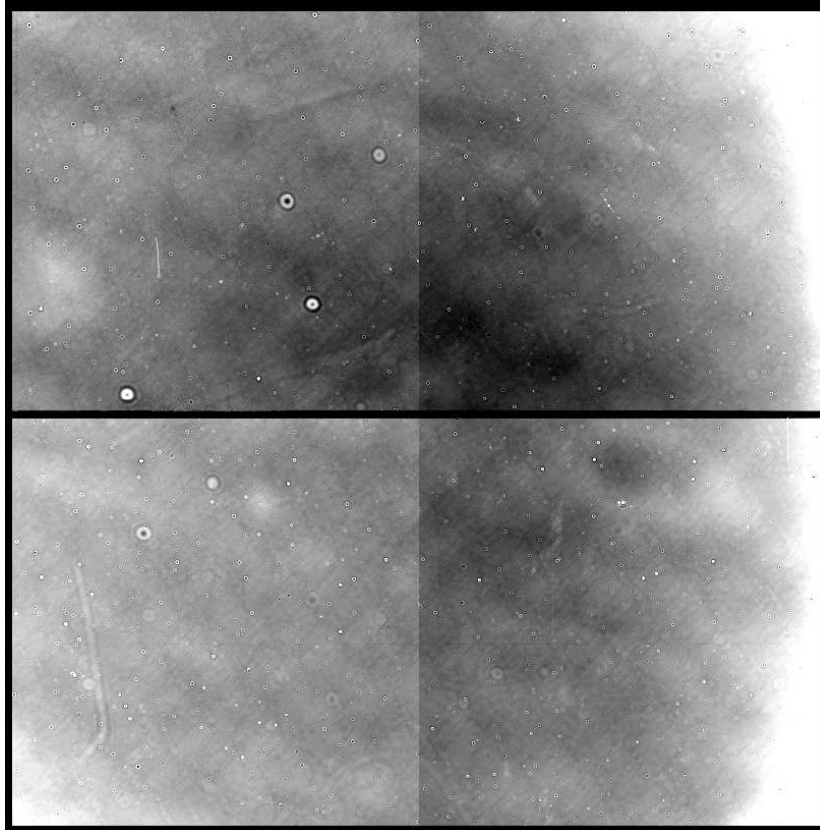
F336W  
D2

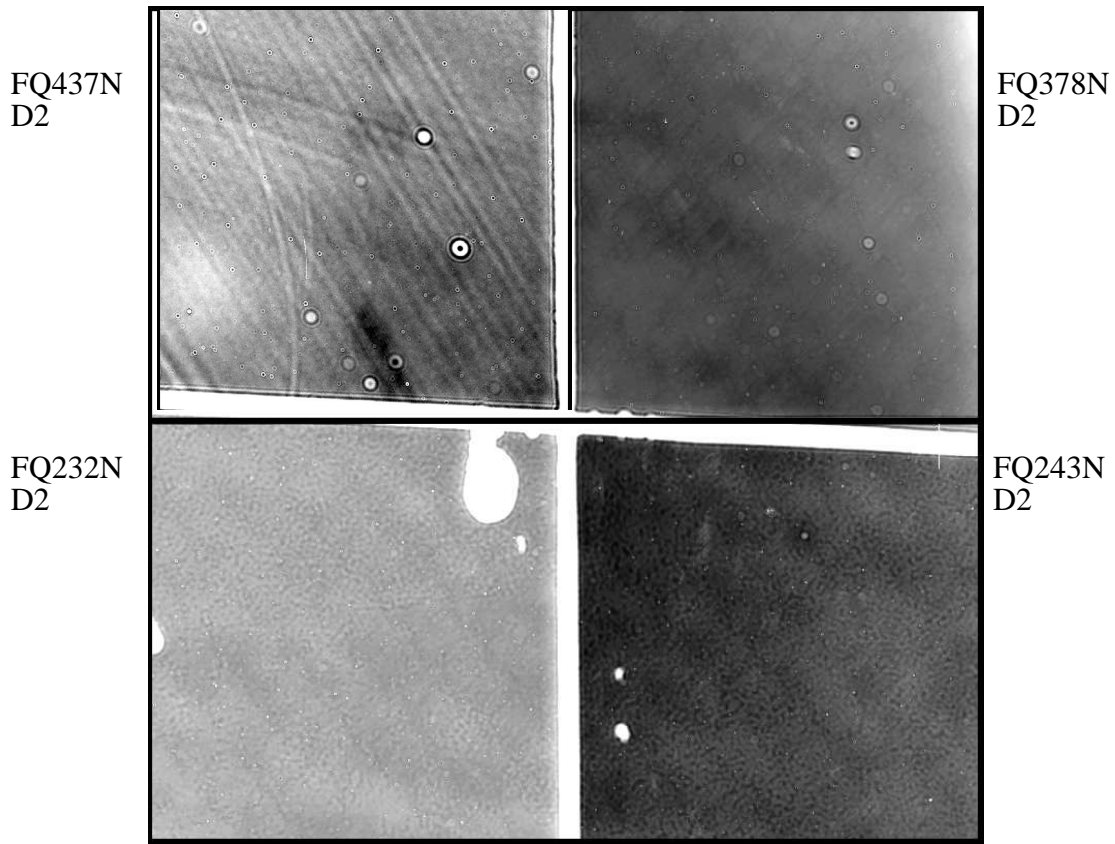


F343N  
D2



F390M  
D2





Note: due to the differences in sensitivity levels in the quad filter, the image for FQ437N had to be displayed and captured separately, then pasted into place later (i.e., borders may not align perfectly with the other quadrants. The black border between A/B is also a cut/paste artifact).